AD NUMBER

AD471246

LIMITATION CHANGES

TO:

Approved for public release; distribution is unlimited.

FROM:

Distribution authorized to U.S. Gov't. agencies and their contractors; Critical Technology; AUG 1965. Other requests shall be referred to Bureau of Naval Weapons, Washington, DC 20360. This document contains export-controlled technical data.

AUTHORITY

APL ltr, 3 Oct 1966

SECURITY MARKING

The classified or limited status of this report applies to each page, unless otherwise marked.
Separate page printouts MUST be marked accordingly.

THIS DOCUMENT CONTAINS INFORMATION AFFECTING THE NATIONAL DEFENSE OF THE UNITED STATES WITHIN THE MEANING OF THE ESPIONAGE LAWS, TITLE 18, U.S.C., SECTIONS 793 AND 794. THE TRANSMISSION OR THE REVELATION OF ITS CONTENTS IN ANY MANNER TO AN UNAUTHORIZED PERSON IS PROHIBITED BY LAW.

NOTICE: When government or other drawings, specifications or other data are used for any purpose other than in connection with a definitely related government procurement operation, the U. S. Government thereby incurs no responsibility, nor any obligation whatsoever; and the fact that the Government may have formulated, furnished, or in any way supplied the said drawings, specifications, or other data is not to be regarded by implication or otherwise as in any manner licensing the holder or any other person or corporation, or conveying any rights or permission to manufacture, use or sell any patented invention that may in any way be related thereto.

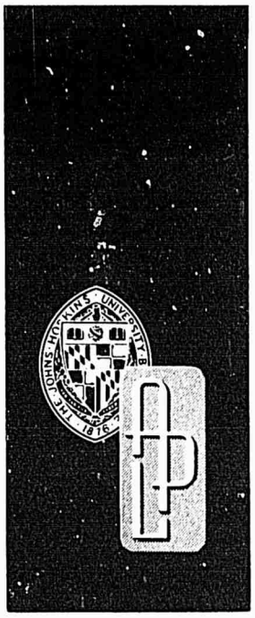

TG–721
AUGUST 1965
Copy No. 37

Technical Memorandum

THERMAL STRESS ANALYSIS OF SANDWICH CYLINDERS

by R. M. RIVELLO

THE JOHNS HOPKINS UNIVERSITY ▪ APPLIED PHYSICS LABORATORY

TG–721
AUGUST 1965

Technical Memorandum

THERMAL STRESS ANALYSIS OF SANDWICH CYLINDERS

by R. M. RIVELLO

**Consultant, Applied Physics Laboratory and
Associate Professor of Aerospace Engineering,
University of Maryland**

THE JOHNS HOPKINS UNIVERSITY ▪ APPLIED PHYSICS LABORATORY
8621 Georgia Avenue, Silver Spring, Maryland 20910

Operating under Contract NOw 62-0604-c, Bureau of Naval Weapons, Department of the Navy

TABLE OF CONTENTS

LIST OF ILLUSTRATIONS

The Johns Hopkins University
APPLIED PHYSICS LABORATORY
Silver Spring, Maryland

SUMMARY

Three theories are developed for computing the thermal stresses in sandwich cylinders with a continuous isotropic core. These are based upon the following idealizations: (1) dividing the cylinder into concentric constant modulus sub-cylinders which are analyzed by thick cylinder theory, (2) treating the faces as membranes and the core as a thick cylinder, and (3) using a modified thin-shell theory which accounts for the variable modulus. Results from the theories are compared for an alumina sandwich which is typical of radome construction. It is found that the thin-shell formulation results in a simple equation but is only accurate at large values of the mean radius to total thickness ratio. The membrane-face equations agree well with the concentric-cylinder theory but computational difficulties are comparable to the latter method. The concentric-thick-cylinder theory has therefore been selected to be programmed for machine computation. It may also be used to analyze homogeneous cylinders in which the modulus is temperature dependent and therefore varies through the wall thickness.

INTRODUCTION

The aerodynamic heating associated with high speed flight produces large temperatures and thermal gradients in missile structures. Refractory materials capable of operating at high temperatures usually have low strength/weight ratios and are therefore structurally inefficient. One method of increasing their structural effectiveness is to employ them in sandwich configurations in which the core material is made porous to decrease its density. As an example, laminated slip cast ceramic radomes are currently under development by several companies. The electrical bandwidth and cost advantages that these radomes appear to hold over homogeneous wall radomes have been discussed in Ref. (1). The structural advantages that such radomes have in resisting aerodynamic and inertial loads are also apparent, but the effectiveness with regard to thermal stresses is not so obvious and requires quantitative investigation. The work reported herein was undertaken to develop the analytical methods to be used in such a study.

Weckesser and Suess have used the cylinder as an analytical model to compare the thermal shock characteristics of various materials for homogeneous wall radomes (Ref. 2). They find that the thermal stresses are critical in the region of transition from laminar to turbulent flow. Since the ratio of the cylinder radius to the wall thickness is small at the transition point they use thick-walled cylinder theory (Ref. 3) to compare stresses. Their results have been found to be in reasonable agreement with limited wind tunnel tests (Ref. 4). The cylindrical configuration was also selected for the sandwich investigation so that the results could be directly compared with the previously determined data for homogeneous wall construction.

The theories which have been considered are based upon the following idealizations of the sandwich cylinder:

1. Dividing the cylinder into concentric sub-cylinders with constant mechanical properties in each region. The regions are then treated as thick-walled cylinders and radial displacements and stresses are matched at their interfaces.

2. The thin faces layers of the sandwich are treated as membranes and the core as a thick-walled cylinder. Radial forces and displacements are matched at the junction of the faces and the core.
3. The sandwich is analyzed by the Love's theory of thin shells modified to include the effects of the non-homogeneity of the wall.

The derivations for the above theories are contained in Appendices A through D. A comparison of the results obtained by using the theories is given in the next section.

RESULTS

In order to obtain a comparison of the accuracy and relative computational difficulties of the three theories, thermal stresses were determined in the sandwich cylinder shown in Figure 1. The geometry and mechanical properties are typical of an alumina sandwich radome having a core with a porosity of 67%. The temperature distribution was taken from Ref. (5) and is shown in Figure 2. Mechanical properties and thermal expansion data for the alumina were obtained from Refs. (6) and (7) assuming that Poisson's ratio and thermal expansion are not affected by porosity.

Circumferential stresses (σ_θ) and axial stresses (σ_z) were computed at the inner radius, and radial stresses (σ_r) were found at the juncture of the inner face with the core by each of the theories. Results are shown in Figure 3 for a range of outside radii assuming the same thermal gradient and wall geometry in all cases.

DISCUSSION

The equations for the concentric thick-walled cylinder are derived in Appendices A and B. The results in Figure 3 were obtained using 3

cylinders, one for each of the face layers and one for the core. This development of the problem utilizes the three-dimensional theory of elastic bodies in both the faces and the core and is therefore the most exact of the three theories. However, it is not convenient to obtain a closed form solution by this method since this would require a general solution of 6 simultaneous linear algebraic equations to evaluate the constants of integration. The analysis is therefore only practical when a digital computer is used to solve the equations for a particular design. The concentric thick-wall cylinder solution is also useful in the analysis of homogeneous cylinders since it is possible to take into account the variation of modulus of elasticity with temperature. This is done by dividing the homogeneous wall into concentric cylinders and evaluating the modulus in each region at the mean temperature for that region.

The membrane face theory derived in Appendix C is restricted to those cases in which the face thicknesses are very small compared to the radius. It assumes that the radial stresses in the faces are negligible compared to the axial and circumferential stresses so that a two-dimensional stress-strain law can be used. It further assumes that the axial and circumferential stresses are constant through the face thicknesses. Uncertainties are introduced into the analysis by lumping the faces into membranes at discrete radii. It is not clear if the radial stresses and displacements of the membrane and core should be matched at the outer surface of the face layer, the center of this layer, or at its interface with the core. The results in Figure 3, which are for the membranes at the interfaces, show good agreement with the more exact concentric cylinder theory over the range of radii investigated. While the membrane-face theory results in a closed form solution the equations are lengthy and time consuming to evaluate.

The non-homogeneous thin shell theory is derived in Appendix D. The development assumes that normals to the reference surface remain normal, straight, and unchanged in length. Radial thermal strains are thereby ignored. Radial stresses are considered negligible compared to the axial

and circumferential stresses throughout the body so that the stress-strain relations are two-dimensional. Equilibrium is only satisfied on a macroscopic scale by the stress resultants rather than on an infinitesimal basis by the stresses. The resulting closed form solution is simple to evaluate but it is seen from Figure 3 that it is grossly in error when the radius to thickness ratio is small. For the case which was studied the error relative to the concentric cylinder solution reduces to 6% for a sandwich mid-radius to total thickness ratio of 5 and is less than 4% for a ratio of 10. It is interesting to note from Appendix D that, except in the edge regions, the stresses in a thin shell of revolution do not depend upon the shape of the shell if the temperature only varies through the thickness. Furthermore, results obtained by using an AVCO computer program (Ref. 8) show that this is also true when the temperature variation in the mendional direction is gradual, in which case the stresses depend only upon the local temperature distribution through the thickness and may be computed from Eq. (D.14).

The behavior displayed by the circumferential and axial stresses in Figure 3 at small radii is interesting. It is seen that the circumferential stresses decrease but that the axial stresses increase. This same situation does not prevail in a homogeneous cylinder where the circumferential and axial stresses are equal regardless of the radius and both increase with a decrease in radius. The reduction of core modulus appears to be effective in decreasing the circumferential stresses since it increases the relative radial motion between the inner and outer faces. However, significant changes do not occur in the relative axial motions except in the edge regions so that the axial stress in the inner face remains high. The lengths of the edge region where reduced axial stresses occur will increase but for the length to thickness ratios used in radomes there will still be a central portion where plane sections remain plane as assumed in the theories. The thin shell theory does not admit to relative radial motions and therefore does not show the reduction of the circumferential stresses for small values of the ratio of mean radius to total thickness.

CONCLUDING REMARKS

Three theories have been developed for the analysis of sandwich cylinders. As would be expected, the modified thin shell theory results in the simplest equation but gives large errors at values of the mean radius to total thickness ratio less than 5. The membrane face theory is in good agreement with the concentric thick cylinder analysis but requires considerable computational effort making it impractical for repeated calculations unless it is programmed for machine computation, in which case the concentric-cylinder analysis is preferable. As a result the theoretical analysis described in Appendices A and B, which is also useful in analyzing homogeneous radomes in which the modulus is temperature dependent, has been selected for machine programming.

On the basis of limited computations it appears that the low modulus core is effective in reducing the circumferential stress at low values of the mean radius to total thickness ratio but that the axial stresses are not decreased.

APPENDIX A

Derivation of Equations for Concentric Thick-Walled Cylinder Theory

The non-homogeneous cylinder is assumed to be divided into concentric sub-cylinders as shown in Figure 4 so that the modulus of elasticity is constant within each layer. To identify the layers they are numbered consecutively from 1 for the inner to n for the outer cylinder. The inner and outer radii of the ith cylinder are designated by b_i and b_{i+1} respectively.

It is assumed that the materials are isotropic and that Poisson's ratio, ν, is constant in all layers. This assumption does not impose severe restrictions on the theory for ν of most structural materials (within the elastic limit) falls between 0.25 and 0.33. For a given material moderate changes in porosity do not affect ν and the temperature dependency is slight so that this assumption is fully justified in sandwich cylinders made of a single material but with different porosities in the various layers. Since E_i is constant in the ith cylinder, we may apply the Duhamel equations (Ref. 3) for thermal deflections and stresses in a homogeneous hollow cylinder to the region. If we assume the ends of the cylinder to be restrained against axial displacement these are given by Eqs. (c) through (f) from page 409 of Ref. (3). For the ith region we obtain

$$u_i = \frac{1+\nu}{1-\nu} \cdot \frac{1}{r} \int_{b_i}^{r} (\alpha T) r dr + C_{i1}\, r + \frac{C_{i2}}{r} \qquad \text{(A-1)}$$

$$\sigma_{r_i} = -\frac{E_i}{1-\nu} \cdot \frac{1}{r^2} \int_{b_i}^{r} (\alpha T) r dr + \frac{E_i}{1+\nu} \left(\frac{C_{i1}}{1-2\nu} - \frac{C_{i2}}{r^2} \right) \qquad \text{(A-2)}$$

$$\sigma_{\theta_i} = \frac{E_i}{1-\nu} \cdot \frac{1}{r^2} \int_{b_i}^{r} (\alpha T) r dr - \frac{(\alpha T) E_i}{1-\nu} + \frac{E_i}{1+\nu} \left(\frac{C_{i1}}{1-2\nu} - \frac{C_{i2}}{r^2} \right) \tag{A-3}$$

$$\sigma_{z_i} = - \frac{(\alpha T) E_i}{1-\nu} + \frac{2\nu E_i C_{i1}}{(1+\nu)(1-2\nu)} \tag{A-4}$$

In these equations C_{i1} and C_{i2} are constants of integration which apply to the ith region.

The coefficient of expansion has been brought under the integral sign in writing these equations since it is always permissible to consider αT (the unrestrained strain due to temperature) as a single quantity. As a result α need not be linear over the range of temperature changes.

Since there are n regions a total of 2n constants of integration must be found. These constants are determined so that equilibrium and compatability are satisfied on the faces and interfaces of the layers. Equilibrium on the inner and outer faces requires that

$$\sigma_{r_i} (b_i) = -p_1 \tag{A-5}$$

and

$$\sigma_{r_n} (b_{n+1}) = -p_{n+1} \tag{A-6}$$

where p_1 and p_{n+1} are the external pressures on the inner and outer faces. At each of the interfaces the equilibrium condition

$$\sigma_{r_i} (b_{i+1}) = \sigma_{r_{i+1}} (b_{i+1}); \; i=1,2,\ldots,(n-1) \tag{A-7}$$

and the compatability condition

$$u_i (b_{i+1}) = u_{i+1} (b_{i+1}); \; i=1,2,\ldots,(n-1) \tag{A-8}$$

must be satisfied. Substituting Eqs. (A-1) and (A-2) into (A-5) through (A-8) gives

$$\left(\frac{1}{1-2\nu}\right) C_{1,1} - \frac{1}{b_1^2} C_{1,2} = - \frac{p_1(1+\nu)}{E_1} \tag{A-9}$$

$$\left(\frac{1}{1-2\nu}\right) C_{n,1} - \frac{1}{b_{n+1}^2} C_{n2} = (1+\nu)\left(\frac{A_n}{b_{n+1}^2} - \frac{p_{n+1}}{E_n}\right) \tag{A-10}$$

$$\left(\frac{1}{1-2\nu}\right) C_{i,1} - \frac{1}{b_{i+1}^2} C_{i,2} - \frac{E_{i+1}}{E_i(1-2\nu)} C_{i+1,1}$$

$$+ \frac{E_{i+1}}{E_i b_{i+1}^2} C_{i+1,2} = (1+\nu) \frac{A_i}{b_{i+1}^2} \; ; \; i=1,2,\ldots,(n-1) \tag{A-11}$$

$$C_{i,1} + \frac{1}{b_{i+1}^2} C_{i,2} - C_{i+1,1} - \frac{1}{b_{i+1}^2} C_{i+1,2}$$

$$= - (1+\nu) \frac{A_i}{b_{i+1}^2} \; ; \; i = 1,2,\ldots, (n-1) \tag{A-12}$$

where

$$A_i = \frac{1}{1-\nu} \int_{b_i}^{b_{i+1}} \alpha T r dr \tag{A-13}$$

Solution of the 2n simultaneous equations generated by Eqs. (A-9) through (A-12) gives the C_{i1} and C_{i2} coefficients. Substitution of these into Eqs. (A-3) and (A-4) yields σ_{θ_i} and σ_{z_i} for restrained ends.

The resultant axial force for restrained ends is

$$R = 2\pi \sum_{i=1}^{n} \int_{b_i}^{b_{i+1}} \sigma_{z_i} \, r dr$$

which by using Eq. (A-4) becomes

$$R = -2\pi \sum_{i=1}^{n} \left[\frac{E_i}{1-\nu} \int_{b_i}^{b_{i+1}} \alpha T r dr - \frac{2\nu E_i C_{i1}}{(1+\nu)(1-2\nu)} \int_{b_i}^{b_{i+1}} r dr \right]$$

From Eq. (A-13) we find

$$\frac{R}{\pi} = -2 \sum_{i=1}^{n} \left[E_i A_i - \frac{\nu E_i C_{i1}}{(1+\nu)(1-2\nu)} (b_{i+1}^2 - b_i^2) \right] \qquad \text{(A-14)}$$

To determine the axial stresses for unrestrained ends we determine the stresses due to an axial force of -R and superimpose these upon the previously determined stresses. The stresses due to -R are (Appendix B, Eq. (B-1)).

$$\sigma_{z_i} = - \frac{E_i R}{\pi \sum_{j=1}^{n} E_j (b_{j+1}^2 - b_j^2)} \; ; \; \sigma_\theta = 0; \; \sigma_r = 0$$

In the ith region the radial and circumferential stresses for unrestrained ends are then given by Eqs. (A-2) and (A-3). The axial stress is

$$\sigma_{z_i} = - \frac{\alpha T E_i}{1-\nu} + \frac{2\nu E_i C_{i1}}{(1+\nu)(1-2\nu)} + \frac{E_i (R/\pi)}{\sum_{j=1}^{n} E_j (b_{j+1}^2 - b_j^2)} \qquad \text{(A-15)}$$

The quantity A_i defined by Eq. (A-13) will usually have to be evaluated by a numerical integration procedure such as Simpson's rule. When the wall thickness of the ith cylinder is small it is sufficiently accurate to assume that αT varies linearly through the thickness so that

$$\alpha T(r) = \frac{1}{(b_{i+1} - b_i)} \left\{ b_{i+1}\, \alpha T(b_i) - b_i \alpha T(b_{i+1}) + \left[\alpha T(b_{i+1}) - \alpha T(b_i)\right] r \right\} \qquad \text{(A-16)}$$

Substituting this into Eq. (A-13) we find for a thin wall

$$A_i = \frac{1}{6(1-\nu)(b_{i+1}-b_i)} \left[\alpha T(b_i)(b_{i+1}^3 - 3b_i^2\, b_{i+1} + 2b_i^3) + \alpha T(b_{i+1})(2b_{i+1}^3 - 3b_i b_{i+1}^2 + b_i^3) \right] \qquad \text{(A-17)}$$

This equation is poorly suited for numerical computations since it results in small differences of large numbers. An equation of improved numerical accuracy may be obtained by substituting the relation $b_{i+1} = b_i + t_i$ (where t_i is the thickness of the wall of the ith cylinder) into Eq. (A-17) which upon simplification becomes

$$A_i = \frac{t_i}{6(1-\nu)} \left[\alpha T(b_i)\, (3b_i + t_i) + \alpha T(b_{i+1})\, (3b_i + 2t_i) \right] \qquad \text{(A-18)}$$

APPENDIX B

Derivation of Equations for Axially Loaded Concentric Thick-Walled Cylinders

In the thermal stress analysis for non-homogeneous cylinders given in Appendix A, the stresses due to an axial load were required. In this appendix we shall show by the inverse method that Eq. (A-15) correctly describes the stresses.

The cylinder, which is the same as described in Appendix A and shown in Figure 4, is assumed to be subjected to normal forces distributed over the ends which have a resultant tensile force R directed parallel to the axis. The cylinder is long so that, except in the immediate vicinity of the ends, a state of generalized plane strain exists. The stresses therefore only depend upon the resultant of the end forces and not upon their distribution. We assume R to be divided among the regions in proportion to their stiffnesses so that

$$\left.\begin{aligned} \sigma_{z_i} &= \frac{E_i R}{\pi \sum_{j=1}^{n} E_j (b_{j+1}^2 - b_j^2)} \\ \sigma_{r_i} &= \sigma_{\theta_i} = \tau_{\theta z_i} = \tau_{z r_i} = 0 \end{aligned}\right\} \qquad \text{(B-1)}$$

describes the stresses in the ith region. These stresses satisfy the equations of equilibrium

$$\frac{\partial \sigma_{r_i}}{\partial r} + \frac{\partial \tau_{r z_i}}{\partial z} + \frac{\sigma_{r_i} - \sigma_{\theta_i}}{r} = 0$$

$$\frac{\partial \tau_{r z_i}}{\partial r} + \frac{\partial \sigma_{z_i}}{\partial z} + \frac{\tau_{r z_i}}{r} = 0$$

which apply to axially symmetrical stress distributions in a solid of revolution (Eqs. 177, Ref. 3). Eqs. (B-1) also satisfy the following compatibility equations (Eq. (g), page 346, Ref. (3)

$$\nabla^2 \sigma_{r_i} - \frac{2}{r^2} (\sigma_{r_i} - \sigma_{\theta_i}) + \frac{1}{1+\nu} \frac{\partial^2 \Theta}{\partial r^2} = 0$$

$$\nabla^2 \sigma_{\theta_i} + \frac{2}{r^2} (\sigma_{r_i} - \sigma_{\theta_i}) + \frac{1}{1+\nu} \cdot \frac{1}{r} \frac{\partial \Theta}{\partial r} = 0$$

$$\nabla^2 \sigma_{z_i} + \frac{1}{1+\nu} \frac{\partial^2 \Theta}{\partial z^2} = 0$$

$$\nabla^2 \tau_{rz_i} - \frac{1}{r^2} \tau_{rz_i} + \frac{1}{1+\nu} \frac{\partial^2 \Theta}{\partial r \partial z} = 0$$

where Θ is the sum of the normal stresses, which from Eqs. (B-1) is equal to σ_{z_i}, and

$$\nabla^2 = \frac{\partial^2}{\partial r^2} + \frac{1}{r} \frac{\partial}{\partial r} + \frac{\partial^2}{\partial z^2}$$

is the Laplacian operator for axial symmetry. The boundary conditions to be satisfied on the cylindrical faces are given in Appendix A by Eqs. (A-5) through (A-8). Eqs. (A-5) through (A-7) are identically satisfied because $\sigma_{r_i} = 0$. Since σ_{z_i} is the only non-zero stress, the strains are given by the uniaxial stress-strain laws

$$\epsilon_{z_i} = \frac{\sigma_{z_i}}{E_i} ; \quad \epsilon_{r_i} = \epsilon_{\theta_i} = -\frac{\nu \sigma_{z_i}}{E_i} \tag{B-2}$$

The strain displacement equations are (Eqs. 178, Ref. 3)

$$\epsilon_{r_i} = \frac{\partial u_i}{\partial r} , \quad \epsilon_{\theta_i} = \frac{u_i}{r} , \quad \epsilon_{z_i} = \frac{\partial w_i}{\partial z} ; \quad \gamma_{rz_i} = \frac{\partial u_i}{\partial z} + \frac{\partial w_i}{\partial r} \tag{B-3}$$

By simultaneously solving Eqs. (B-1) through (B-3) we find the displacements to be

$$u_i = \frac{\nu R r}{\pi \sum_{j=1}^{n} E_j (b_{j+1}^2 - b_j^2)} \qquad (B\text{-}4)$$

$$w_i = \frac{R z}{\pi \sum_{j=1}^{n} E_j (b_{j+1}^2 - b_j^2)}$$

The first of these equations satisfies the remaining boundary condition (A-8) at each of the interfaces of the cylindrical surfaces. The second equation indicates that, as supposed, plane sections remain plane. Finally we see Eqs. (B-1) satisfy the equation

$$R = 2\pi \sum_{i=1}^{n} \int_{b_i}^{b_{i+1}} \sigma_{z_i} \, r dr$$

thereby assuring a state of equilibrium between the applied force R and the internal stresses

APPENDIX C

Derivation of Equations for Membrane-Face Theory

In sandwich structures the face layers are often thin compared to the core layer. This suggests a simplified theory in which the faces are treated as membranes while the core is analyzed as a thick-walled cylinder. The geometry and notation are shown in Figure 5. The following assumptions are made.

(1) The temperatures in the face layers are uniform through their thicknesses. These temperatures are designated T_1 and T_3; the moduli E_1 and E_3 are determined at the corresponding temperatures. Average temperatures are used when there are gradients through the face layers.

(2) The only stresses of importance in the membrane faces are σ_θ and σ_z, and these stresses are constant through the membrane thicknesses.

(3) The core region 2 is a "thick" cylinder, i.e. the effects of radial stresses are considered.

(4) The temperature distribution in the core is arbitrary but E_2 is constant and is evaluated at the mean temperature of region 2.

(5) The membrane stiffnesses are lumped at a and b, the inner and outer radii of the core respectively.

As a result of assumption (3) the deflections and stresses in the core for restrained ends are given by Eqs. (c) through (f), page 409 of Ref. (3), which are

$$u = \frac{1+\nu}{1-\nu} \cdot \frac{1}{r}\int_a^r \alpha T r dr + C_1 r + \frac{C_2}{r} \qquad \text{(C-1)}$$

$$\sigma_r = -\frac{E_2}{1-\nu} \cdot \frac{1}{r^2}\int_a^r \alpha T r dr + \frac{E_2}{1+\nu}\left(\frac{C_1}{1-2\nu} - \frac{C_2}{r^2}\right) \qquad \text{(C-2)}$$

$$\sigma_\theta = \frac{E_2}{1-\nu} \cdot \frac{1}{r^2}\int_a^r \alpha T r dr - \frac{\alpha T E_2}{1-\nu} + \frac{E_2}{1+\nu}\left(\frac{C_1}{1-2\nu} - \frac{C_2}{r^2}\right) \tag{C-3}$$

$$\sigma_z = -\frac{\alpha T E_2}{1-\nu} + \frac{2\nu E_2 C_1}{(1+\nu)(1-2\nu)} \tag{C-4}$$

From Eqs. (C-1) and (C-2), the radial displacements and stresses at a and b are given by

$$u(a) = C_1 a + \frac{C_2}{a} \tag{C-5}$$

$$u(b) = (1+\nu)\frac{A}{b} + C_1 b + \frac{C_2}{b} \tag{C-6}$$

$$\sigma_r(a) = \frac{E_2}{1+\nu}\left(\frac{C_1}{1-2\nu} - \frac{C_2}{a^2}\right) \tag{C-7}$$

$$\sigma_r(b) = -\frac{E_2 A}{b^2} + \frac{E_2}{1+\nu}\left(\frac{C_1}{1-2\nu} - \frac{C_2}{b^2}\right) \tag{C-8}$$

where

$$A = \frac{1}{1-\nu}\int_a^b \alpha T r dr \tag{C-9}$$

Because of assumption (2) the strains in the inner face are given by the two-dimensional stress-strain equations

$$\left.\begin{aligned} \epsilon_{\theta_1} &= \frac{1}{E_1}\left(\sigma_{\theta_1} - \nu\sigma_{z_i}\right) + (\alpha T)_1 \\ \epsilon_{z_i} &= \frac{1}{E_1}\left(\sigma_{z_i} - \nu\sigma_{\theta_1}\right) + (\alpha T)_1 \end{aligned}\right\} \tag{C-10}$$

where ν is assumed to be the same as for the core. With restrained ends $\epsilon_z = 0$ and it follows from the second of Eqs. (C-10) that

$$\sigma_{z_1} = \nu\sigma_{\theta_1} - (\alpha T)_1 E_1 \tag{C-11}$$

Substituting this into the first of Eq. (C-10) gives

$$\epsilon_{\theta_1} = \frac{(1-\nu^2)}{E_1} \sigma_{\theta_1} + (1+\nu)(\alpha T)_1 \tag{C-12}$$

The circumferential strain in the inner membrane face is related to its radial displacement u_1 by

$$\epsilon_{\theta_1} = \frac{u_1}{a} \tag{C-13}$$

The radial stress in the core at r = a imposes a bursting pressure on the inner membrane so that σ_{θ_1} is given by the hoop stress equation

$$\sigma_{\theta_1} = \frac{pR}{t} = \frac{\left[\sigma_r(a) + p_1\right] a}{t_1}$$

where p_1 is the inside pressure.
From Eq. (C-7) this may be written

$$\sigma_{\theta_1} = \frac{E_2 a}{t_1(1+\nu)} \left(\frac{C_1}{1-2\nu} - \frac{C_2}{a^2} \right) + \frac{p_1 a}{t_1} \tag{C-14}$$

In a similar fashion, for the outer face we find

$$\sigma_{\theta_3} = \frac{E_2 A}{b t_3} - \frac{E_2 b}{t_3(1+\nu)} \left(\frac{C_1}{1-2\nu} - \frac{C_2}{b^2} \right) - \frac{p_3 b}{t_3} \tag{C-15}$$

where p_3 is the outside pressure.

By combining Eqs. (C-12) through (C-14) we obtain

$$u_i = a\left[\frac{E_2 a}{E_1 t_1}\ (1-\nu)\ \left(\frac{C_1}{1-2\nu} - \frac{C_2}{a^2}\right) + \frac{p_1 a}{E_1 t_1}\ (1-\nu^2) + (1+\nu)\ (\alpha T)_1\right] \qquad \text{(C-16)}$$

and by the same procedure the radial displacement of the outer face is

$$u_3 = b\left[(1-\nu^2)\ \frac{E_2 A}{E_3 t_3 b} - (1-\nu)\ \frac{E_2 b}{E_3 t_3}\left(\frac{C_1}{1-2\nu} - \frac{C_2}{1-2\nu}\right) - \frac{p_3 b}{E_3 t_3}\ (1-\nu^2)+(1+\nu)(\alpha T)_3\right] \qquad \text{(C-17)}$$

Noting that $u_1 = u(b)$ for compatible deformations of the faces and core we find the following simultaneous equations for C_1 and C_2 by equating Eqs. (C-5) with (C-16) and (C-6) with (C-17)

$$DC_1 + EC_2 = J$$

$$FC_1 + GC_2 = K$$

where

$$D = a^2\left[1 - \frac{E_2 a}{E_1 t_1}\ \frac{(1-\nu)}{(1-2\nu)}\right]$$

$$E = 1 + \frac{E_2 a}{E_1 t_1}\ (1-\nu)$$

$$F = b^2\left[1 + \frac{E_2 b}{E_3 t_3}\ \frac{(1-\nu)}{(1-2\nu)}\right]$$

$$G = 1 - \frac{E_2 b}{E_3 t_3}\ (1-\nu)$$

$$J = (1+\nu)\left[a^2 (\alpha T)_1 + \frac{p_1 a^3}{E_1 t_1}\ (1-\nu)\right]$$

$$K = (1+\nu)\left[b^2 (\alpha T)_3 - \frac{p_3 b^3}{E_3 t_3}\ (1-\nu) - AG\right]$$

Solving the simultaneous equations leads to the results

$$\left.\begin{aligned} C_1 &= (JG - EK)/(DG - EF) \\ C_2 &= (DK - FJ)/(DG - EF) \end{aligned}\right\} \quad \text{(C-18)}$$

The σ_z stresses in the core for restrained ends are obtained by substituting C_1 into Eq. (C-4). The resultant restraining force in the core is found by integrating Eq. (C-4) over the core area so that

$$R_2 = 2\pi \int_a^b \sigma_z \, r dr$$

$$= - 2\pi \left[E_2 A - \frac{\nu E_2 C_1 (b^2 - a^2)}{(1+\nu)(1-2\nu)} \right]$$

For restrained ends, the axial stress in the inner face is found by substituting Eq. (C-14) into Eq. (C-11) giving

$$\sigma_{z_1} = \frac{\nu a E_2}{(1+\nu) t_1} \left(\frac{C_1}{1-2\nu} - \frac{C_2}{a^2} \right) - (\alpha T)_1 E_1 \quad \text{(C-19)}$$

which produces a resultant force

$$R_1 = 2\pi a t_1 \left[\frac{\nu E_2 a}{(1+\nu) t_1} \left(\frac{C_1}{1-2\nu} - \frac{C_2}{a^2} \right) - (\alpha T)_1 E_1 \right]$$

In a similar fashion we find

$$\sigma_{z_3} = \frac{\nu E_2}{t^3} \left[\frac{A}{b} - \frac{b}{1+\nu} \left(\frac{C_1}{1-2\nu} - \frac{C_2}{b^2} \right) \right] - (\alpha T)_3 E_3 \quad \text{(C-20)}$$

$$R_3 = 2\pi b t_3 \left[\frac{\nu E_2 A}{t_3 b} - \frac{\nu E_2 b}{(1+\nu) t_3} \left(\frac{C_1}{1-2\nu} - \frac{C_2}{b^2} \right) - (\alpha T)_3 E_3 \right]$$

The total restraining force is then

$$R = R_1 + R_2 + R_3$$

which gives

$$\frac{R}{\pi} = -2\left[(1-\nu)E_2A + (\alpha T)_1E_1at_1+(\alpha T)_3E_3bt_3\right] \tag{C-21}$$

The stresses for unrestrained ends are determined by superimposing the stresses for an axial load of -R. By following the method of Appendix B we find these stresses to be

$$\left.\begin{aligned} \sigma_z &= \frac{E_i(R/\pi)}{2E_1at_1+E_2(b^2-a^2)+2E_3bt_3} \\ \sigma_r &= \sigma_\theta = 0 \end{aligned}\right\} \tag{C-22}$$

The total stresses for unrestrained ends are obtained by substituting the stresses from Eqs. (C-22) upon the previously determined stresses for restrained ends. The results are: for the inner face

$$\left.\begin{aligned} \sigma_{\theta_1} &= \frac{E_2a}{(1+\nu)t_1}\left(\frac{C_1}{1-2\nu} - \frac{C_2}{a^2}\right) \\ \sigma_{z_1} &= \frac{\nu E_2a}{(1+\nu)t_1}\left(\frac{C_1}{1-2\nu} - \frac{C_2}{a^2}\right) - (\alpha T)_1E_1 - \frac{E_1(R/\pi)}{2E_1at_1+E_2(b^2-a^2)+2E_3bt_3} \end{aligned}\right\} \tag{C-23}$$

for the outer face

$$\left.\begin{aligned}
\sigma_{\theta_3} &= \frac{E_2 b}{t_3}\left[\frac{A}{b^2} - \frac{1}{1+\nu}\left(\frac{C_1}{1-2\nu} - \frac{C_2}{b^2}\right)\right] \\
\sigma_{z_3} &= \frac{\nu E_2 b}{t_3}\left[\frac{A}{b^2} - \frac{1}{1+\nu}\left(\frac{C_1}{1-2\nu} - \frac{C_2}{b^2}\right)\right] - (\alpha T)_3 E_3 \\
&\quad - \frac{E_3(R/\pi)}{2E_1 a t_1 + E_2(b^2-a^2) + 2E_3 b t_3}
\end{aligned}\right\} \quad (C\text{-}24)$$

and for the core

$$\left.\begin{aligned}
\sigma_{r_2} &= -\frac{E_2}{1-\nu} \cdot \frac{1}{r^2}\int_a^r \alpha T r dr + \frac{E_2}{1+\nu}\left(\frac{C_1}{1-2\nu} - \frac{C_2}{r^2}\right) \\
\sigma_{\theta_2} &= \frac{E_2}{1-\nu} \cdot \frac{1}{r^2}\int_a^r \alpha T r dr - \frac{(\alpha T)E_2}{1-\nu} + \frac{E_2}{1+\nu}\left(\frac{C_1}{1-2\nu} + \frac{C_2}{r^2}\right) \\
\sigma_{z_2} &= -\frac{(\alpha T)E_2}{1-\nu} + \frac{2\nu E_2 C_1}{(1+\nu)(1-2\nu)} - \frac{E_2(R/\pi)}{2E_1 a t_1 + E_2(b^2-a^2) + 2E_3 b t_3}
\end{aligned}\right\} \quad (C\text{-}25)$$

APPENDIX D

Derivation of Equations for Nonhomogeneous Shell Theory

In this appendix the equations for the stresses and displacements in a nonhomogeneous thin shell of revolution subjected to a temperature distribution which only varies through the thickness are derived. The nonhomogeneity is assumed to occur in the thickness direction only.

The thermal stresses give rise to the stress resultants shown in Figure 6. These are defined as follows

$$\left.\begin{aligned} N_\varphi &= \int_h \sigma_\varphi \, dz & N_\theta &= \int_h \sigma_\theta \, dz \\ M_\varphi &= \int_h \sigma_\varphi \, z d\varphi & M_\theta &= \int_h \sigma_\theta \, z dz \\ Q_\varphi &= \int_h \tau_{\psi z} \, dz \end{aligned}\right\} \qquad (D.1)$$

where φ and θ are coordinates shown in Figure 7 and z is a coordinate measured from, and normal to the reference surface (defined later) of the shell. The integrals extend over the shell thickness h.

Force and moment equilibrium conditions for the differential element of Figure 6 lead to the following equations (pp. 534, Ref. 9)

$$\frac{d}{d\varphi}(N_\varphi r_o) - N_\theta r_1 \cos\varphi - r_o Q_\varphi + r_o r_1 Y = 0$$

$$N_\varphi r_o + N_\theta r_1 \sin\varphi + \frac{d(Q_\varphi r_o)}{d\varphi} + Z r_1 r_o = 0$$

$$\frac{d}{d\varphi}(M_\varphi r_o) - M_\theta r_1 \cos\varphi - Q_\varphi r_1 r_o = 0$$

where the radii r_o and r_1 are shown in Figure 7. No external loading is applied so that the surface forces Y and Z in these equations are zero.

The material is considered to be linearly elastic. In addition the following assumptions which are usual in shell theory are made: (a) the material is isotropic in the surface of the shell, (b) the modulus of elasticity in the z direction and the shear modulus which relates $\tau_{z\varphi}$ to $\gamma_{z\varphi}$ are infinite, and (c) the coefficient of expansion in the z direction, and the Poisson's ratio which relates the strain in the z direction to the strains in the surface directions of the shell are zero. This is equivalent to the Kirchoff assumptions that normals to the reference surface remain normal and unchanged in length during deformation of the shell. As a result the plane-stress Hooke's law equations

$$\left.\begin{aligned} \epsilon_\varphi &= \frac{1}{E}\,(\sigma_\varphi - \nu\sigma_\theta) + \alpha T \\ \epsilon_\theta &= \frac{1}{E}\,(\sigma_\theta - \nu\sigma_\varphi) + \alpha T \end{aligned}\right\} \qquad (D.3)$$

apply. Solving these for the stresses gives

$$\left.\begin{aligned} \sigma_\varphi &= \frac{E}{1-\nu^2}\,(\epsilon_\varphi + \nu\epsilon_\theta) - \frac{\alpha E T}{1-\nu} \\ \sigma_\theta &= \frac{E}{1-\nu^2}\,(\epsilon_\theta + \nu\epsilon_\varphi) - \frac{\alpha E T}{1-\nu} \end{aligned}\right\} \qquad (D.4)$$

Using the previously mentioned shell assumptions that normals to the reference surface remain normal and unchanged in length during deformation of the shell, the strains may be expressed as (p. 431, Ref. 9)

$$\left.\begin{aligned} \epsilon_\varphi &= \epsilon_\varphi(0) - \chi_\varphi z \\ \epsilon_\theta &= \epsilon_\theta(0) - \chi_\theta z \end{aligned}\right\} \qquad (D.5)$$

where $\epsilon_\varphi(0)$ and $\epsilon_\theta(0)$ are the strains in the reference surface (z=0) and χ_φ and χ_θ are the changes of curvature of the reference surface.

Placing these into Eq. (D.4) gives

$$\sigma_\varphi = \frac{E}{1-\nu^2}\left[\epsilon_\varphi(0) + \nu\epsilon_\theta(0) - z\,(\chi_\varphi + \nu\chi_\theta)\right] - \frac{\alpha ET}{1-\nu}$$

$$\sigma_\theta = \frac{E}{1-\nu^2}\left[\epsilon_\theta(0) + \nu\epsilon_\varphi(0) - z\,(\chi_\theta + \nu\chi_\varphi)\right] - \frac{\alpha ET}{1-\nu}$$

By substituting the equation for σ_φ into the relationship for N_φ and M_φ from Eqs. (D.1) we find

$$\left.\begin{aligned} N_\varphi &= \frac{1}{1-\nu^2}\left[\epsilon_\varphi(0) + \nu\epsilon_\theta(0)\right]\int_h E\,dz - \frac{1}{1-\nu^2}\,(\chi_\varphi + \nu\chi_\theta)\int_h zE\,dz - \frac{1}{1-\nu}\int_h \alpha ET\,dz \\ M_\varphi &= \frac{1}{1-\nu^2}\left[\epsilon_\varphi(0) + \nu\epsilon_\theta(0)\right]\int_h zE\,dz - \frac{1}{1-\nu^2}\,(\chi_\varphi + \nu\chi_\theta)\int_h z^2E\,dz - \frac{1}{1-\nu}\int_h \alpha ETz\,dz \end{aligned}\right\} \quad (D.6)$$

where it is assumed that E may vary through the shell thickness. These equations are simplified if z is measured from a surface such that $\int_h zE\,dz = 0$. The distance to this surface from an arbitrary initial surface is given by

$$\bar{z}' = \frac{\int_h z_o \frac{E}{E_1}\,dz}{\int_h \frac{E}{E_1}\,dz} \quad (D.7)$$

where z_o is the distance measured from the arbitrary initial surface and E_1 is an arbitrarily chosen reference modulus. When E is piecewise constant within layers of the shell the last equation may be written

$$\bar{z}' = \frac{\sum_{i=1}^{n} z_{o_i}\,\frac{E_i}{E_1}\,h_i}{\sum_{i=1}^{n} \frac{E_i}{E_1}\,h_i} \quad (D.8)$$

In this E_i is the modulus in the ith layer which has a thickness h_i. The distance z_{o_i} is measured to the middle surface of the ith layer and the sums extend over all layers. We note that $\bar{z}'$ is the distance to the modulus-weighted centroidal surface. When the shell is homogeneous $\bar{z}'$ reduces to $\bar{z}$, the distance to the middle surface of the shell.

Measuring z from the reference surface Eqs. (D.6) become

$$N_\varphi = K' \left[\epsilon_\varphi(0) + \nu\epsilon_\theta(0) \right] - \frac{N_T}{1-\nu} \tag{D.9a}$$

$$M_\varphi = -D' \left(\chi_\varphi + \chi_\theta \right) - \frac{M_T}{1-\nu} \tag{D.9b}$$

and in a similar fashion

$$N_\theta = K' \left[\epsilon_\theta(0) + \nu\epsilon_\varphi(0) \right] - \frac{N_T}{1-\nu} \tag{D.9c}$$

$$M_\theta = -D' \left(\chi_\theta + \nu\chi_\varphi \right) - \frac{M_T}{1-\nu} \tag{D.9d}$$

where the following definitions apply

$$\left.\begin{aligned} K' &= \frac{E_1}{1-\nu^2} \int_h \frac{E}{E_1}\, dz, & D' &= \frac{E_1}{1-\nu^2} \int_h z^2 \frac{E}{E_1}\, dz \\ N_T &= \int_h \alpha E T dz, & M_T &= \int_h \alpha E T z dz \end{aligned}\right\} \tag{D.10}$$

The quantities K' and D' are the extensional and bending rigidities of the nonhomogeneous shell. When E is piecewise constant in layers the first two of Eqs. (D.10) may be written

$$\begin{aligned} K' &= \frac{E_1}{1-\nu^2} \sum_{i=1}^{n} \frac{E_i}{E_1} h_i \\ D' &= \frac{E_i}{1-\nu^2} \sum_{i=1}^{n} \frac{E_i}{E_1} \left(\frac{h_i^3}{12} + z_i^2 h_i \right) \end{aligned} \tag{D.11}$$

When the shell is homogeneous, K' and D' reduce to K and D, the usual shell stiffnesses defined by (Ref. 9)

$$K' = K = \frac{Eh}{1-\nu^2} \quad , \quad D' = D = \frac{Eh^3}{12(1-\nu^2)}$$

The displacement of an arbitrary point in the reference surface is resolved into two components: v which is tangent to the meridian through the point and w in the direction of the inward normal to the reference surface (Figure 8). The strains and changes of curvature of the reference surface may be expressed in terms of the displacements as follows (pp. 534 - 535, Ref. (9)

$$\left.\begin{aligned} \epsilon_\varphi(0) &= \frac{1}{r_1}\frac{dv}{d\varphi} - \frac{w}{r_1}, \quad \epsilon_\theta(0) = \frac{v}{r_2}\cot\varphi - \frac{w}{r_2} \\ \chi_\varphi &= \frac{1}{r_1}\frac{d}{d\varphi}\left(\frac{v}{r_1} + \frac{dw}{r_1 d\varphi}\right), \quad \chi_\theta = \left(\frac{v}{r_1} + \frac{dw}{r_1 d\varphi}\right)\frac{\cot\varphi}{r_2} \end{aligned}\right\} \quad (D.12)$$

where r_2 is the principal radius of curvature shown in Figure 7. Substituting Eqs. (D.12) into (D.9) we find

$$\left.\begin{aligned} N_\varphi &= K'\left[\frac{1}{r_1}\frac{dv}{d\varphi} - \frac{w}{r_1} + \nu\left(\frac{v}{r_2}\cot\varphi - \frac{w}{r_2}\right)\right] - \frac{N_T}{1-\nu} \\ N_\theta &= K'\left[\frac{v}{r_2}\cot\varphi - \frac{w}{r_2} + \nu\left(\frac{1}{r_1}\frac{dv}{d\varphi} - \frac{w}{r_1}\right)\right] - \frac{N_T}{1-\nu} \\ M_\varphi &= -D'\left[\frac{1}{r_1}\frac{d}{d\varphi}\left(\frac{v}{r_1} + \frac{dw}{r_1 d\varphi}\right) + \nu\left(\frac{v}{r_1} + \frac{dw}{r_1 d\varphi}\right)\frac{\cot\varphi}{r_2}\right] - \frac{M_T}{1-\nu} \\ M_\theta &= -D'\left[\left(\frac{v}{r_1} + \frac{dw}{r_1 d\varphi}\right)\frac{\cot\varphi}{r_2} + \frac{\nu}{r_1}\frac{d}{d\varphi}\left(\frac{v}{r_1} + \frac{dw}{r_1 d\varphi}\right)\right] - \frac{M_T}{1-\nu} \end{aligned}\right\} \quad (D.13)$$

By substituting these into Eqs. (D.2) the equilibrium equations may be expressed in terms of v, w, and Q_φ. A solution to these equations is then the solution to the problem.

The solution for the stresses in a homogeneous clamped flat plate of uniform thickness subjected to a temperature distribution which only varies through the thickness is the same as for a cylinder or sphere with the same thickness and temperature distribution (Ref. 9). One would therefore suspect that the stress would be the same for any shell of revolution and that a similar situation may also be true for nonhomogeneous plates and shells.

The thermal stresses in a nonhomogeneous plate with clamped edges and constant K', D', N_T, and M_T is (Ref. 10)

$$\sigma_x = \sigma_y = \frac{E}{1-\nu}\left(\frac{1}{1-\nu^2}\cdot\frac{N_T}{K'} - \alpha T\right), \quad \sigma_z = \tau_{xy} = \tau_{yz} = \tau_{zx} = 0$$

One would be led to believe that

$$\sigma_\varphi = \sigma_\theta = \frac{E}{1-\nu}\left(\frac{1}{1-\nu^2}\cdot\frac{N_T}{K'} - \alpha T\right), \quad \sigma_z = \tau_{\varphi\theta} = \tau_{\theta z} = \tau_{z\varphi} = 0 \qquad \text{(D.14)}$$

may be the solution for a nonhomogeneous shell of revolution in which K', D', N_T, and M_T are constant. It will be shown that this is true.

The stress resultants associated with Eq. (D.14) are found by substituting them into Eqs. (D.1), to give

$$N_\varphi = N_\theta = 0$$

$$M_\varphi = M_\theta = -\frac{M_T}{1-\nu} \qquad \text{(D.15)}$$

$$Q_\varphi = 0$$

These identically satisfy the first two of Eqs. (D.2) and the third reduces to

$$-\frac{M_T}{1-\nu}\left(\frac{dr_o}{d\varphi} - r_1\cos\varphi\right) = 0$$

From Figure 9 we see that if there is no discontinuity in the tangent to the meridian curve $dr_o = r_1 \cos\varphi \, d\varphi$, or

$$\frac{dr_o}{d\varphi} - r_1 \cos\varphi = 0$$

so that the last equation is also identically satisfied and Eq. (D.14) is the solution.

The deflections are found by integrating the strains. By substituting Eq. (D.14) into (D.3) we find

$$\varepsilon_\varphi = \varepsilon_\theta = \frac{1}{1-\nu^2} \cdot \frac{N_T}{K'}$$

which, from the first 2 of Eqs. (D.12) gives

$$\left.\begin{aligned} \frac{1}{r_1}\frac{dv}{d\varphi} - \frac{w}{r_1} &= \frac{1}{1-\nu^2} \cdot \frac{N_T}{K'} \\ \frac{v}{r_2}\cot\varphi - \frac{w}{r_2} &= \frac{1}{1-\nu^2} \cdot \frac{N_T}{K'} \end{aligned}\right\} \quad (D.16)$$

By eliminating w from these equations we obtain the following differential equation for v

$$\frac{dv}{d\varphi} - v\cot\varphi = \frac{1}{1-\nu^2} \frac{N_T}{K'} (r_1 - r_2) \quad (D.17)$$

Integrating (pp. 446 - 447, Ref. 9) we find

$$v = \sin\varphi \left[\frac{1}{1-\nu^2} \cdot \frac{N_T}{K'} \int \frac{(r_1 - r_2)\, d\varphi}{\sin\varphi} + C \right]$$

where C is a constant of integration to be determined from the known value of v at the support. By substituting Eq. (D.17) into the second of Eqs. (D.16) the following equation for w is obtained

$$w = \frac{1}{1-\nu^2} \cdot \frac{N_T}{K'} \left\{ \cos\varphi \left[\int \frac{(r_1 - r_2)\, d\varphi}{\sin\varphi} + C \right] - r_2 \right\} \quad (D.18)$$

REFERENCES

1. Loyet, D. L. and Yoshitami, R. Ceramic Sandwich Radome Design, Proc. of the OSU-RTD Symposium on Electromagnctic Windows, Vol. III, 2-4 June 1964.
2. Weckesser, L. B. and Suess, R. P., Limitations of Radome Materials, Quarterly Report, Research and Exploratory Development for the Missile Guidance and Airframe Branch Bureau of Naval Weapons, JHU/APL, Oct-Dec, 1964.
3. Timoshenko, S. and Goodier, J. N., Theory of Elasticity, McGraw-Hill Book Co., Inc., New York, 1951.
4. Suess, R. P., Comparison of Theory and Experiment, Radome Temperatures and Stresses, JHU/APL EM-3884, 1 July 1964.
5. Suess, R. P., Temperature Analyses of Solid Wall Alumina and Alumina A-Sandwich Radomes, JHU/APL EM-3980, July 1965.
6. Coble, D. L. and Weckesser, L. B., Electrical, Mechanical, and Thermal Properties of Alumina, Fused Silica, and Pyroceram 9606, JHU/APL EM-3926. Dec. 7, 1964.
7. Lynch, J. F., et al, Refractory Ceramics of Interest in Aerospace Structural Applications - A Materials Selection Handbook, RTD-TDR-63-4102, Supplement 1, May 1964.
8. Radkowski, P. P., Davis, R. M., and Bolduc, M. R., Numerical Analysis of Thin Shells of Revolution, ARS Jor., Jan. 1962, pp. 36-41.
9. Timoshenko, S. and Woinowsky - Krieger, S., Theory of Plates and Shells, McGraw-Hill Book Co., Inc., New York, 1959.
10. Rivello, R. M., An Introduction to the Analysis of Flight Structures, Unpublished Lecture Notes Dept. of Aerospace Engineering, Univ. of Md., 1962.

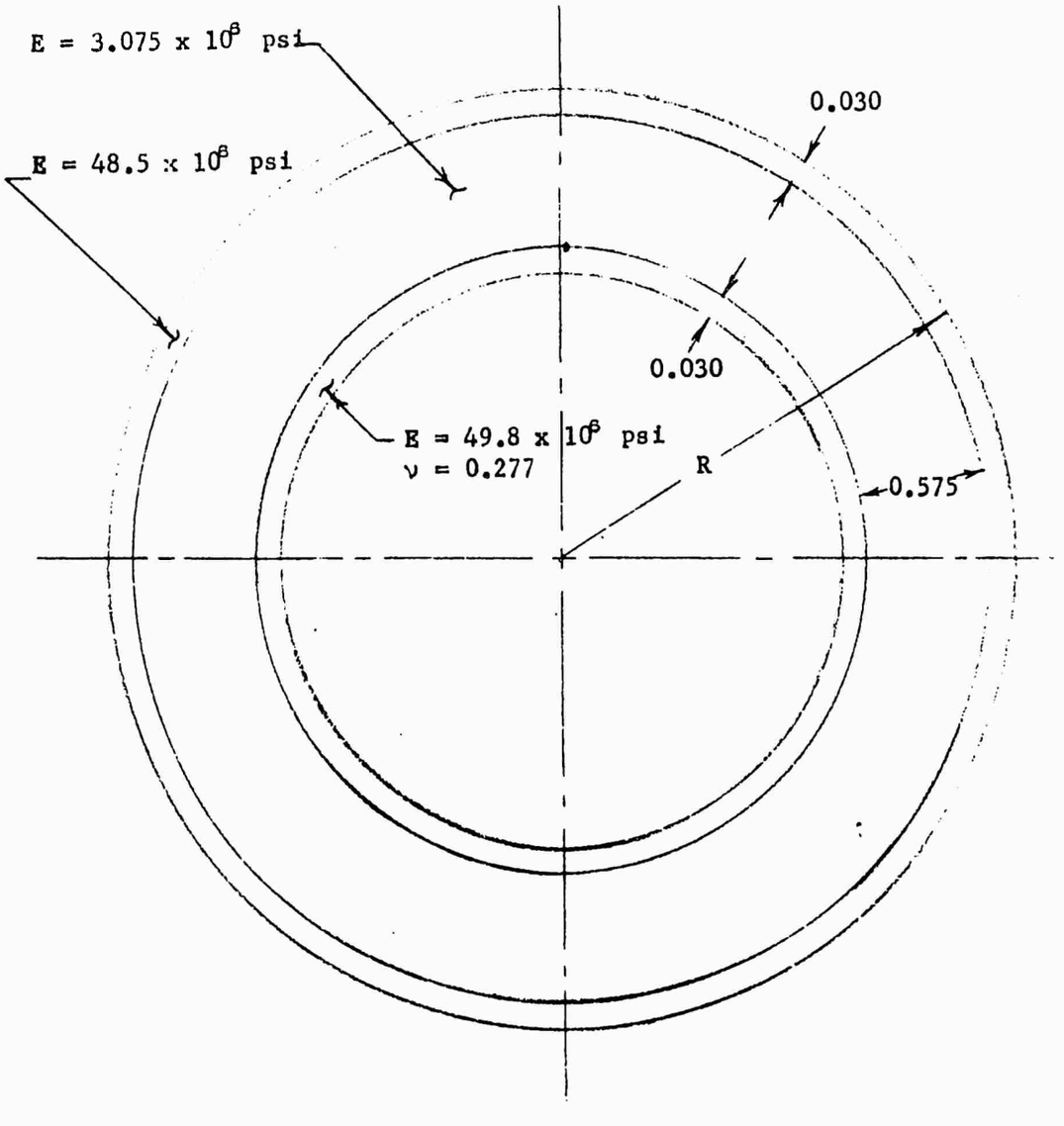

Fig. 1 SANDWICH CYLINDER TYPICAL OF ALUMINA RADOME.

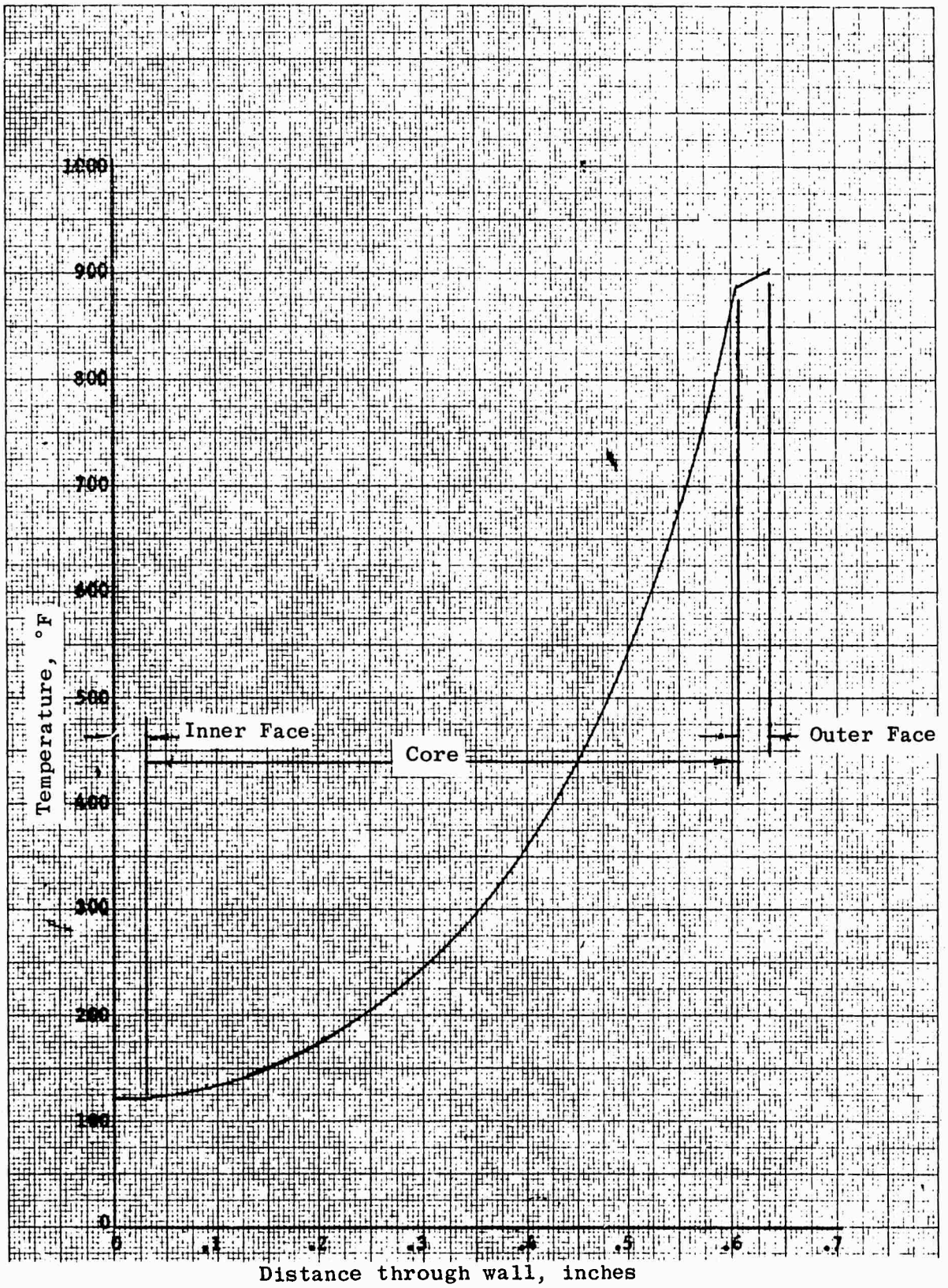

Fig. 2 TEMPERATURE DISTRIBUTION.

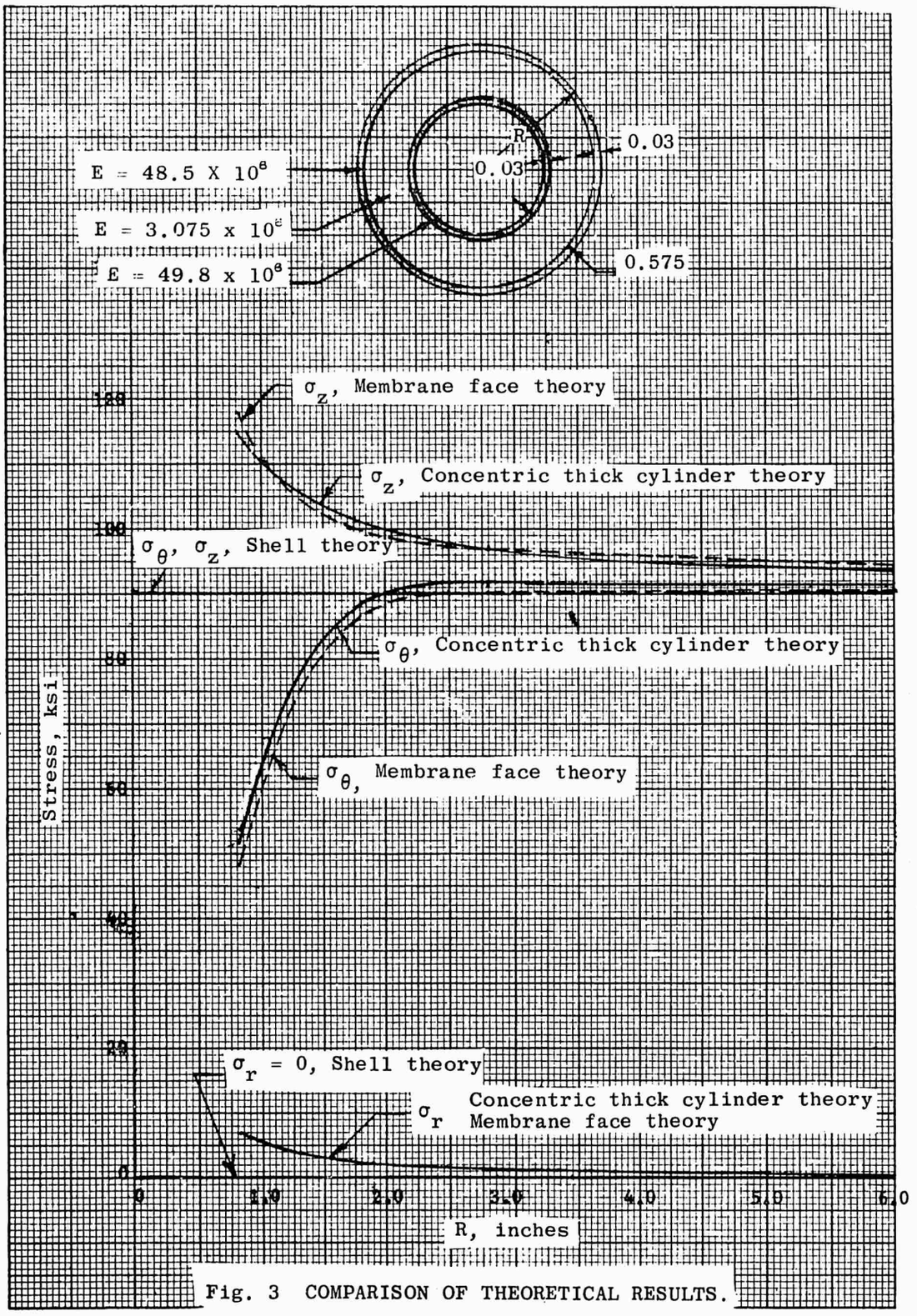

Fig. 3 COMPARISON OF THEORETICAL RESULTS.

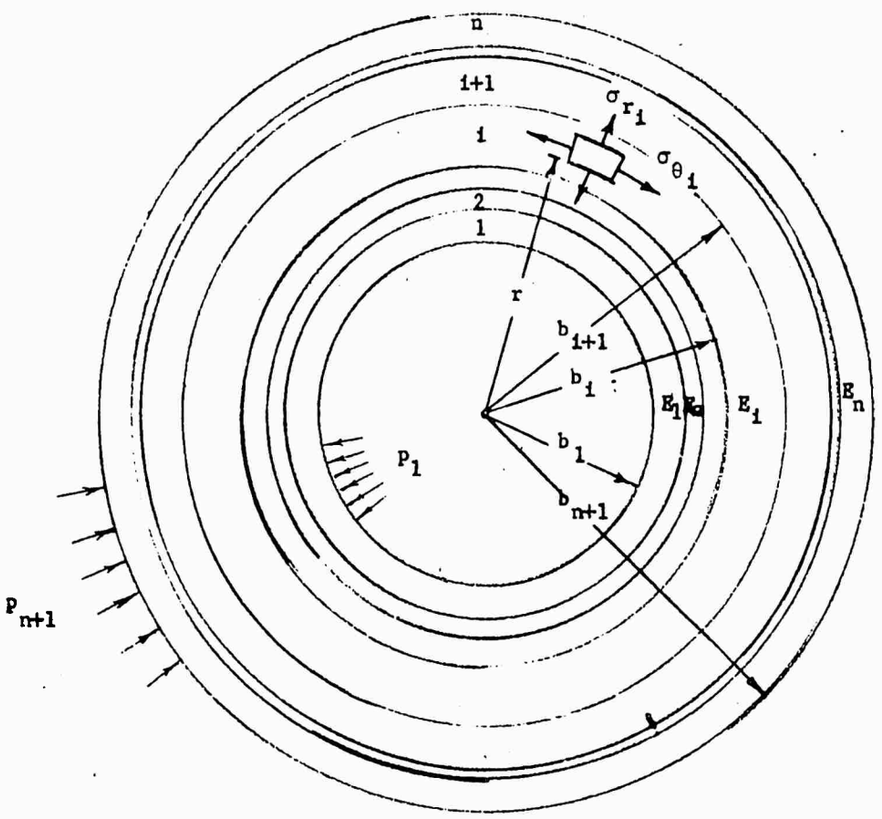

Fig. 4 GEOMETRY AND NOTATION FOR CONCENTRIC THICK WALL CYLINDER THEORY.

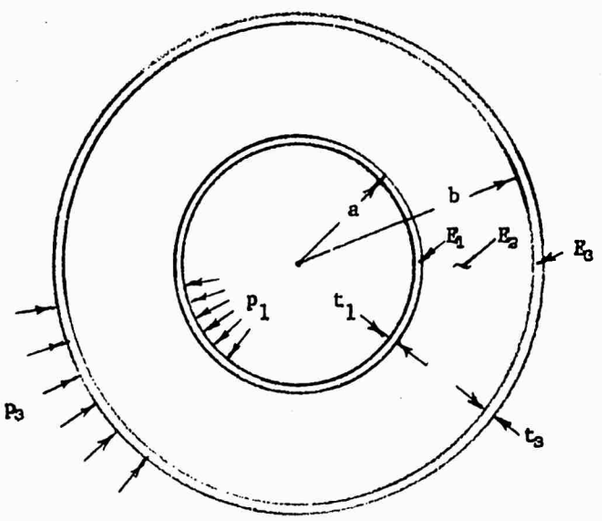

Fig. 5 GEOMETRY AND NOTATION FOR MEMBRANE-FACE THEORY.

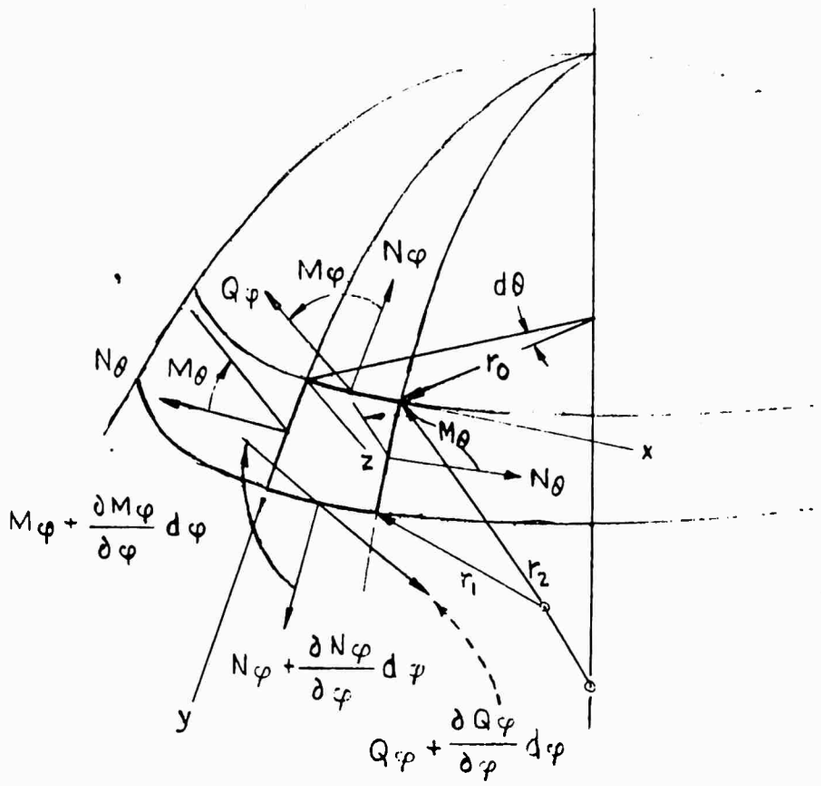

Fig. 6 GEOMETRY AND STRESS-RESULTANTS IN A THIN SHELL OF REVOLUTION.

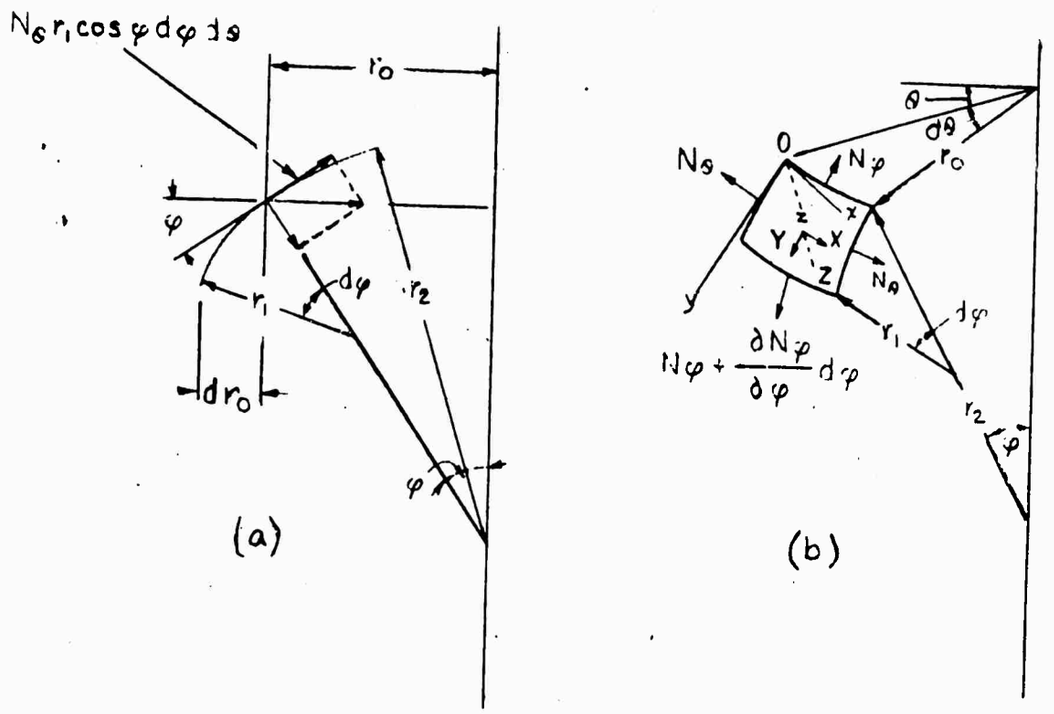

Fig. 7 COORDINATES AND GEOMETRY OF A THIN SHELL OF REVOLUTION.

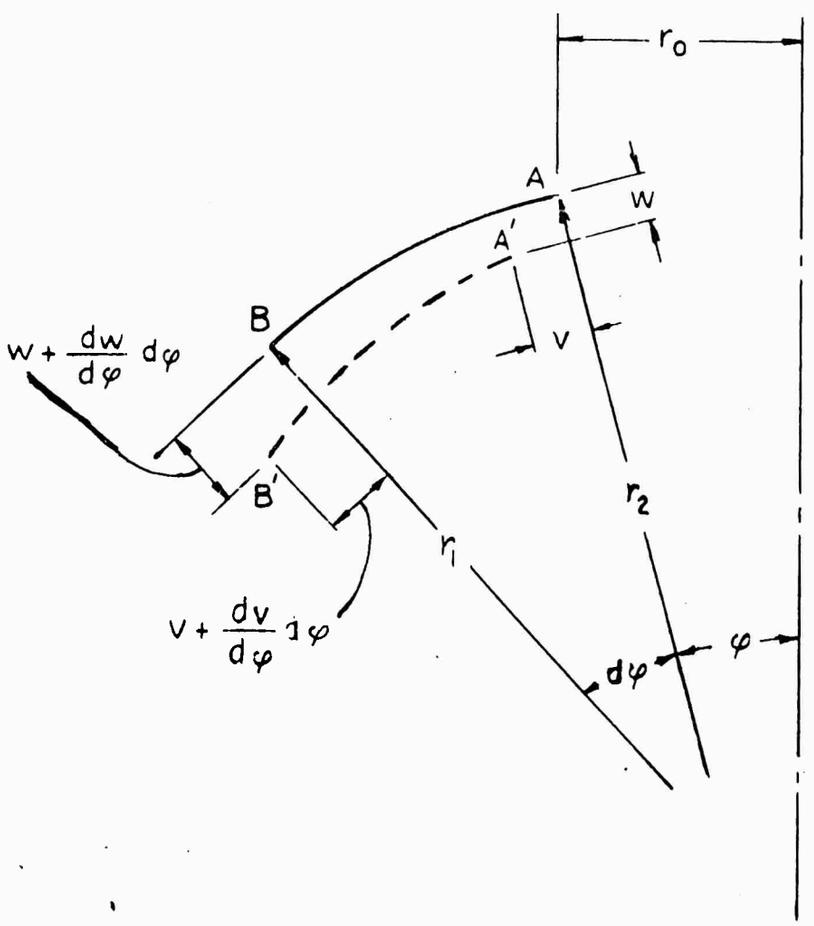

Fig. 8 DISPLACEMENT OF A THIN SHELL OF REVOLUTION.

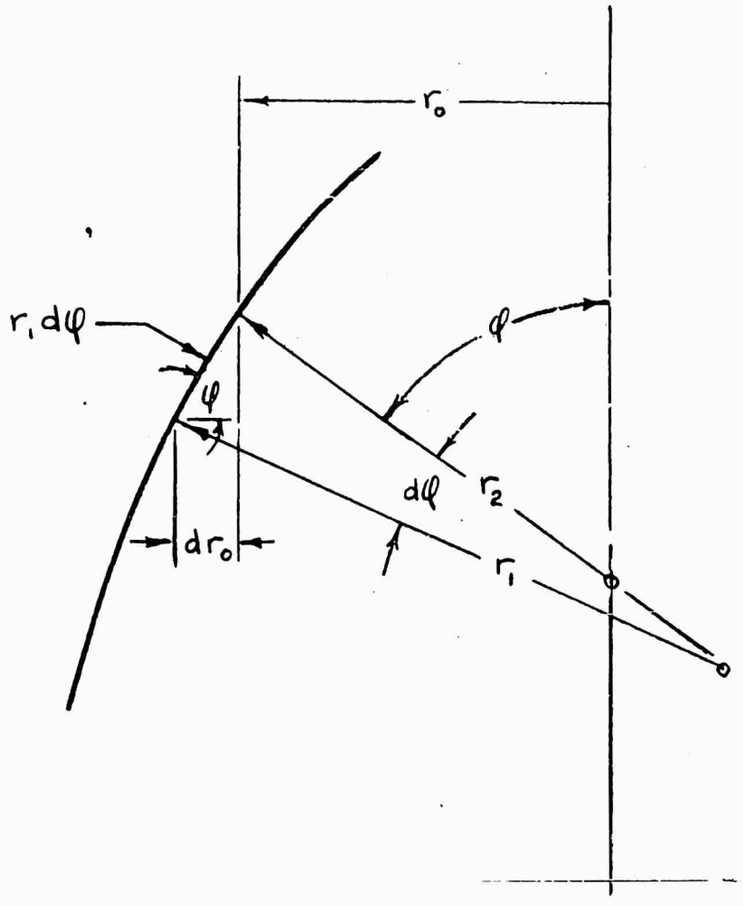

Fig. 9 GEOMETRY SHOWING THAT $dr_o = (r_1\ d\varphi) \cos \varphi$.

INITIAL DISTRIBUTION EXTERNAL TO THE APPLIED PHYSICS LABORATORY*

The work reported in TG 721 was done under Bureau of Naval Weapons Contract NOw-62-0604-c (Task A33) supported by BuWeps RMGA.

ORGANIZATION	LOCATION	ATTENTION	No. of Copies
DEPARTMENT OF DEFENSE			
DDC	Alexandria, Va.		20
Department of the Navy			
Chief, BuWeps	Washington, D. C.	DLI-31	2
		RMGA	1
		RMGA-811	1
BuWepsRep	Silver Spring, Md.		1
NOTS	China Lake, Cal.	W. J. Werbeck	1
CONTRACTORS			
GD/P	Pomona, Cal.	W. Herbig	1
		D. Maytubby	1

*Initial distribution of this document within the Applied Physics Laboratory has been made in accordance with a list on file in the APL Technical Reports Group.